THE DISTRIBUTION OF CHROMIUM ON MERCURY'S SURFACE. L. R. Nittler[1,*], E. Crapster-Pregont[2], E. A. Frank[1], T. J. McCoy[3], F. M. McCubbin[4], Richard D. Starr[5,6], K. E. Vander Kaaden[7], A.Vorburger[2,8], S. Z. Weider[1], [1]Department of Terrestrial Magnetism, Carnegie Institution of Washington, Washington, DC 20015, USA, [2]Department of Earth and Planetary Sciences, American Museum of Natural History, New York, NY 10024, USA, [3]National Museum of Natural History, Smithsonian Institution, Washington, DC 20013, USA, [4]NASA Johnson Space Center, Houston, TX 77058, USA, [5]Physics Department, The Catholic University of America, Washington, DC 20064, USA, [6]Solar System Exploration Division, NASA Goddard Space Flight Center, Greenbelt, MD 20771, USA, [7]Jacobs, NASA JSC, Houston, TX 77058, USA, [8]Physics Institute, University of Bern, Bern, Switzerland. *E-mail: lnittler@ciw.edu

Introduction: The MErcury Surface, Space ENvironment, GEochemistry, and Ranging (MESSENGER) spacecraft orbited Mercury from March 2011 to April 2015, returning a wealth of data from its instrument payload. The X-Ray Spectrometer (XRS) and Gamma-Ray and Neutron Spectrometer (GRNS) were used to measure and map the surface elemental composition, with the goal of better understanding the origin and geologic evolution of the innermost planet. MESSENGER data revealed that Mercury's crust is enriched in Mg and depleted in Al, Ca, and Fe, relative to other terrestrial planets, and that it is surprisingly rich in volatile elements, including S, Na, K, Cl, and C [1–5]. Moreover, maps of elemental abundances and neutron absorption have revealed the presence of a number of distinct geochemical terranes [6, 7], including a large area enriched in Mg, S, Ca, and Fe and depleted in Al (the 'High Magnesium Region,' HMR), whose origin remains unclear [8, 9].

The XRS detected X-ray fluorescence, induced by incident X-rays emitted from the Sun's corona, from the top tens of micrometers of Mercury's surface. Like Fe, Cr was detectable by XRS during large solar flares [5]. However, due to its low abundance (<1 wt%), and hence low signal to noise ratio, accurate measurement of Cr is difficult and more susceptible to systematic errors than other elements measured by the XRS [3, 5]. Thus, Cr data have previously been reported for only 11 XRS measurements [5]. Here we report a map of Cr across Mercury's surface, based on data acquired through the complete MESSENGER mission. The map reveals spatial heterogeneity of Cr, which correlates with other geochemical parameters.

Methods: We examined all XRS flare spectra previously used to make elemental maps of Mercury [7, 10] and selected 133 spectra to generate a Cr/Si map. Selected spectra had non-zero derived Cr abundances and did not exhibit anomalously high detector backgrounds at high energy. As previously seen [5], the derived Cr/Si ratios show a strong dependence on phase (Sun-planet-XRS) angle, due to shadowing effects. As in [5], we used a linear fit to a plot of Cr/Si versus phase angle to empirically correct for this effect, but this procedure leads to ambiguity in the overall normalization. Here we fixed the average of the corrected Cr/Si values to be 0.003 (corresponding to ~0.08 wt% or 800 ppm of Cr), a factor of 2.3 times lower than the value of 0.007 adopted in [5]. Our choice of a lower value is based on the low-phase-angle end of the trend as these data should be the least affected by shadowing effects [11]. We note that this choice is somewhat arbitrary, and there is at least a factor of two systematic uncertainty in the absolute Cr/Si values. Relative differences between mapped Cr/Si values, however, are much more certain. The relative scatter in corrected Cr/Si values is ~30% (one standard deviation), indicating that the flare-to-flare reproducibility of the Cr/Si measurements is no worse than this. We used the same procedure described by Weider et al. [5, 7] to generate a Cr/Si map from the 133 flare measurements and corresponding footprints on Mercury's surface.

Results and Discussion: Our Cr/Si map is compared to other XRS-derived element ratio maps of Mercury's surface in Figure 1. Coverage in the northern hemisphere is sparse for Cr/Si but the map includes multiple flare measurements across the previously defined HMR and Caloris Basin (CB) geochemical terranes. The observed variability in Cr/Si across the southern hemisphere is statistically marginal, but the HMR—especially its northern, most Mg-rich part—has a clear enrichment in Cr compared with the surrounding intermediate terrane (IT). On average, this northern part of the HMR has Cr/Si=1.8±0.4 times that of the IT (~0.0054 with our adopted normalization). Conversely, the CB interior plains have a low Cr/Si ratio, with an average value of 0.0016 (0.54±0.11 times the IT value). Thus, Cr on Mercury appears to correlate with Mg, S, Ca, and Fe, and anti-correlate with Al, at least in large geochemical terranes. Unfortunately, there are almost no Cr measurements on the northern smooth plains, which show a range of chemical compositions.

Reported MESSENGER XRS and GRNS geochemical results have already been used to investigate possible mineral assemblages and geochemical histories of Mercury's surface materials [12–16]. For instance, it has previously been found—based on the earlier, limited Cr dataset—that Cr is mostly like to exist in sulfides on Mercury's surface [15, 16]. Although the good Cr-S correlation observed here

is consistent with those findings, our derived Cr/Si ratios are generally lower than those used in the calculations of [15]. We will report updated normative mineralogies, by accounting for the new Cr values (but we expect the effect to be relatively small).

The new Cr data may also help to constrain oxygen fugacity (fO_2) on Mercury. Each of the three possible Cr valence states (i.e., Cr^0, Cr^{2+}, and Cr^{3+}) has a distinct geochemical compatibility, with Cr^{2+} the most incompatible (i.e., most easily liberated by minerals into melt during partial melting). For example, lunar basalts, which have fO_2 near IW-1 and $Cr^{2+}/\sum Cr = 0.8 \pm 0.1$ [17], typically have approximately 5200 ± 700 ppm Cr [18]. In contrast, terrestrial MORB typically has only 250 ± 165 ppm [19] Cr at an fO_2 of IW+3.5 and $Cr^{2+}/\sum Cr = 0.31 \pm 0.05$ [17]. Although Cr incompatibility reaches a theoretical maximum at $Cr^{2+}/\sum Cr = 1$, with further drop in fO_2, the stability of Cr^0 increases as the fO_2 value of the Cr-Cr_2O_3 reaction is approached. The aubrites—highly reduced achondrites, thought to have equilibrated at approximately IW-5 [20]—have average Cr abundances of only 200 ppm [21]. The average surface abundance of 800 ppm Cr on Mercury may thus indicate that the source regions of the mercurian lavas were at a higher fO_2 than those of the aubrites. This would be consistent both with the elevated Fe abundances on Mercury compared with the aubrites [5] and the upper range of current fO_2 estimates for Mercury [22]. Alternatively, the aubrite parent body and Mercury could have dissimilar bulk Cr abundances and the differences do not correlate to differences in fO_2.

References: [1] Nittler L. R., et al. (in press) The chemical composition of Mercury, in: S.C. Solomon, L.R. Nittler and B. Anderson (Eds.), Mercury: The view after MESSENGER, Cambridge University Press, Cambridge. [2] Peplowski P. N., et al. (2011) *Science, 333,* 1850–1852. [3] Nittler L. R., et al. (2011) *Science, 333,* 1847–1850. [4] Peplowski P. N., et al. (2014) *Icarus, 228,* 86–95. [5] Weider S. Z., et al. (2014) *Icarus, 235,* 170–186. [6] Peplowski P. N., et al. (2015) *Icarus, 253,* 346–363. [7] Weider S. Z., et al. (2015) *EPSL, 416,* 109–120. [8] Frank E. A., et al. (2017) *JGR: Planets, 122,* 614–632 [9] Mojzsis S. J., et al. (2018) *EPSL, 482,* 536-544. [10] Nittler L. R., et al. (2016) *LPS, 47,* abstract 1237. [11] Maruyama Y., et al. (2008) *Earth, Plan., & Space, 60,* 293–297. [12] Stockstill-Cahill K. R., et al. (2012) *JGR: Planets, 117,* E00L15. [13] Charlier B., et al. (2013) *EPSL, 363,* 50–60. [14] Namur O., et al. (2016) *EPSL, 439,* 117–128. [15] Vander Kaaden K. E., et al. (2017) *Icarus, 285,* 155–168. [16] McCoy T. J., et al. (in press) The geochemical and mineralogical diversity of Mercury, in: S.C. Solomon, L.R. Nittler and B. Anderson (Eds.), Mercury: The View after MESSENGER, Cambridge University Press, Cambridge. [17] Bell A. S., et al. (2014) *Am. Min., 99,* 1404-1412. [18] Delano J. W. (1986) *JGR, 91,* D201-D213. [19] Lehnert K., et al. (2000) *G Cubed, 1,* 1012. [20] McCoy T. J. and Bullock E. S. (2017) Differentiation under highly-reducing conditions: New insights from enstatite meteorites and Mercury, in: L.T. Elkins-Tanton and B.P. Weiss (Eds.), Planetesimals: early Differentiation and Consequences for Planets, Cambridge University Press, Cambridge, 2017. [21] Keil K. (2010) *Chem. Der Erde, 70,* 295-317. [22] McCubbin F. M., et al. (2017) *JGR: Planets, 122,* 2053-2076.

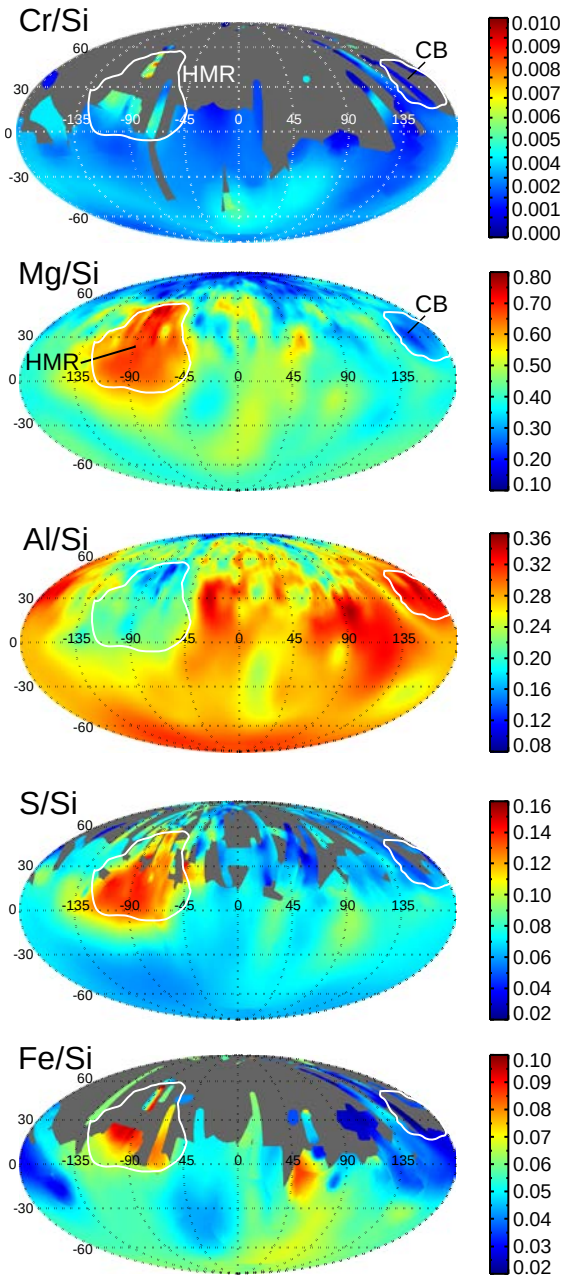

Figure 1. XRS-derived maps of element ratios across Mercury's surface, in Mollweide projection. Outlines of the high magnesium region (HMR) and the Caloris Basin (CB) are shown on Cr/Si map.